Loss of G2A promotes macrophage accumulation in atherosclerotic lesions of low density lipoprotein receptor-deficient mice

Brian W. Parks,* Ginger P. Gambill,* Aldons J. Lusis,† and Janusz H. S. Kabarowski[1],*

Department of Microbiology,* University of Alabama, Birmingham, AL 35294-2170; and Department of Medicine,† University of California, Los Angeles, CA 90095-1679

Abstract **Lysophosphatidylcholine (LPC) is considered a major proatherogenic component of oxidized low density lipoprotein based on its proinflammatory actions in vitro. LPC stimulates macrophage and T-cell chemotaxis via the G protein-coupled receptor G2A and may thus promote inflammatory cell infiltration during atherosclerotic lesion development. However, G2A also mediates proapoptotic effects of LPC and may therefore promote the death of inflammatory cells within developing lesions. To determine how these effects of LPC modify atherogenesis, we examined atherosclerotic lesion development in G2A-sufficient and G2A-deficient low density lipoprotein receptor knockout mice. Although LPC species capable of activating G2A-dependent responses were increased during lesion development, G2A-deficient mice developed lesions similar in size to those in their G2A-sufficient counterparts. Loss of G2A during atherosclerotic lesion development did not reduce macrophage and T-cell infiltration but instead resulted in increased lesional macrophage content associated with reduced numbers of terminal deoxynucleotidyl transferase-mediated dUTP nick end labeled cells and decreased collagen deposition. These data indicate that the ability of LPC to stimulate macrophage and T-cell chemotaxis via G2A is not manifested in vivo and that G2A-mediated proapoptotic rather than chemotactic action is most penetrant during atherogenesis and may modify the stability of atherosclerotic lesions by promoting macrophage death.**—Parks, B. W., G. P. Gambill, A. J. Lusis, and J. H. S. Kabarowski. **Loss of G2A promotes macrophage accumulation in atherosclerotic lesions of low density lipoprotein receptor-deficient mice.** ***J. Lipid Res.*** **2005.** 46: **1405–1415.**

Supplementary key words atherosclerosis • lysophosphatidylcholine • T cells • chemotaxis • apoptosis

Atherosclerosis is an inflammatory disease characterized by the subendothelial accumulation of oxidized low density lipoprotein (OxLDL) in the arterial wall (1). Proinflammatory actions of OxLDL are mediated to a large extent by its phospholipid components. For example, hydrolysis of oxidized phosphatidylcholine decomposition products by lipoprotein-associated platelet-activating factor-acetylhydrolase (PAF-A7H) generates the bioactive lysophospholipid lysophosphatidylcholine (LPC) during LDL oxidation (2). Proinflammatory actions of LPC on cultured macrophages and endothelial cells have led to the widely held view that it is a key proatherogenic component of OxLDL. Most notably, LPC is believed to contribute directly to the recruitment of inflammatory cells during atherosclerotic lesion development. For example, LPC induces intercellular adhesion molecule-1 and monocyte chemotactic protein-1 expression in endothelial cells (3, 4) and stimulates macrophage and T-cell chemotaxis in vitro (5). Although these and many other in vitro studies have provided insights into potential proatherogenic effects of LPC, most have remained poorly characterized mechanistically, as it has been difficult to distinguish nonspecific effects of LPC from those mediated by specific proximal effectors. Furthermore, the multiplicity of cellular and biochemical factors associated with atherosclerotic lesion development raises questions regarding the relevance of these potential atherogenic mechanisms in vivo. However, the recent identification of the G protein-coupled receptor (GPCR) G2A as an effector of LPC action (6–11) has provided a mechanistic framework with which to establish how LPC modifies atherosclerosis independently of its nonspecific actions.

In vitro studies show that G2A induces diverse biologi-

Manuscript received 1 March 2005 and in revised form 28 March 2005.

Published, JLR Papers in Press, April 16, 2005.
DOI 10.1194/jlr.M500085-JLR200

Abbreviations: ESI-MS/MS, electrospray ionization-tandem mass spectrometry; FCS, fetal calf serum; GPCR, G protein-coupled receptor; GPR4, G protein-coupled receptor 4; LDLR$^{-/-}$, low density lipoprotein receptor knockout; LPC, lysophosphatidylcholine; MPO, myeloperoxidase; OGR1, ovarian cancer G protein-coupled receptor 1; OxLDL, oxidized low density lipoprotein; PAF-AH, platelet-activating factor-acetylhydrolase; TDAG8, T-cell death-associated gene 8; TUNEL, terminal deoxynucleotidyl transferase-mediated dUTP nick end labeling.

[1] To whom correspondence should be addressed.
e-mail: janusz@uab.edu

cal effects in response to, as well as independently of, exogenously added LPC. These effects include actin cytoskeleton reorganization and focal adhesion assembly (12, 13), LPC stimulation of macrophage and T-cell chemotaxis (7–9, 11), LPC-dependent extracellular signal regulated kinase mitogen-activated protein kinase activation (11, 14), and LPC-mediated apoptosis (6). Although G2A was originally described as a binding receptor for LPC (14), we have been unable to reproduce the G2A/LPC binding originally reported in crude cell homogenates prepared from receptor-overexpressing cell lines as a result of the high nonspecific membrane binding of this lysophospholipid (14, 15; our unpublished data). Although we cannot rule out a direct interaction between G2A and LPC, a recent study has provided strong evidence for LPC-dependent mobilization of intracellular G2A pools to the plasma membrane as the molecular mechanism by which LPC activates cellular responses via G2A (11). Furthermore, the human G2A receptor and three GPCRs related by sequence homology [G protein-coupled receptor 4 (GPR4), ovarian cancer G protein-coupled receptor 1 (OGR1), and T-cell death-associated gene 8 (TDAG8)] have recently been described as "proton-sensing" receptors (16–18). However, a subsequent comparative study of each receptor confirmed GPR4, OGR1, and TDAG8 as bona fide proton-sensing GPCRs yet failed to detect pH-dependent activation of murine G2A and reported very weak responses of human G2A to extracellular acidification compared with those of GPR4, OGR1, and TDAG8 (19). Thus, there is no evidence to support a proton-sensing function for murine G2A in addition to its role as an effector of LPC action, and the physiological significance of the weak pH sensitivity of the human receptor is questionable and requires further study.

Although G2A-mediated effects of LPC have the potential to modify inflammatory events during atherosclerotic lesion development, their significance in vivo has not been tested. By breeding G2A-deficient mice onto the LDL receptor knockout ($LDLR^{-/-}$) background, we directly assessed the role of G2A in atherosclerosis development. G2A deficiency resulted in increased lesional macrophage numbers associated with decreased apoptosis and reduced collagen content. Thus, G2A deficiency promotes macrophage accumulation, likely by suppressing the death-inducing effects of LPC, which in turn may promote lesion destabilization caused by increased levels of macrophage-derived collagen-degrading enzymes.

MATERIALS AND METHODS

Primary cell isolation and culture

Adherent murine peritoneal macrophages were isolated by culturing peritoneal exudates in DMEM containing 10% fetal calf serum (FCS) for 6 h. Thioglycolate-elicited peritoneal macrophages were obtained from peritoneal exudates of mice injected intraperitoneally 3 days earlier with 3 ml of 4% thioglycolate. All bone marrow-derived cells were cultured from total mononuclear bone marrow cells flushed from the femurs and tibias of mice. Bone marrow cells were cultured at 10^6/ml in DMEM, 10% FCS, 20% L cell-conditioned medium as a source of macrophage-colony stimulating factor, 50 μM 2-mercaptoethanol, 2 mM L-glutamine, 100 U/ml penicillin, and 100 μg/ml streptomycin for 5 days to obtain CD11b-positive macrophages. Bone marrow cells were cultured at 10^6/ml in DMEM, 10% FCS, 50 ng/ml recombinant granulocyte/macrophage-colony stimulating factor, 250 U/ml recombinant interleukin-4, 50 μM 2-mercaptoethanol, 2 mM L-glutamine, 100 U/ml penicillin, and 100 μg/ml streptomycin for 10 days with three medium changes to obtain CD11c-positive dendritic cells. Surface FcεR1 IgE receptor-positive mast cells were generated from bone marrow cells cultured at 10^6/ml in RPMI, 10% FCS, 20% WEHI-3B cell conditioned medium as a source of interleukin-3, 2 mM L-glutamine, 100 U/ml penicillin, and 100 μg/ml streptomycin for 5 weeks with regular medium changes. Platelet/edothelial cell adhesion molecule-1 (PECAM-1)-positive murine endothelial cells were obtained by incubating dissected aorta on Matrigel (BD Biosciences) with DMEM, 10% FCS, 90 μg/ml heparin, 60 μg/ml endothelial cell growth supplement (Collaborative Biomedical Products), 1% Fungizone, 100 U/ml penicillin, and 100 μg/ml streptomycin for 3 days with daily addition of fresh medium. Fifty percent confluent cultures were passaged by dispase treatment onto 100 mm tissue culture plates and incubated until confluent. α-Actin-positive murine aortic smooth muscle cells were cultured from aorta digested with 15 mM HEPES containing 2% BSA, 0.125 μg/ml elastase, 0.25 μg/ml soybean trypsin inhibitor, and 10 μg/ml collagenase D. Aortic digests were forced through a 70 μm filter and cultured in DMEM, 10% FCS, 100 U/ml penicillin, and 100 μg/ml streptomycin until ~80% confluent. $B220^+$ B-cells and $CD4^+$ and $CD8^+$ T-cells were purified from spleens and lymph nodes of mice by immunomagnetic depletion of B-cells (MACS CD45R MicroBeads; Miltenyi Biotec GmbH) followed by incubation with either phycoerythrin-conjugated anti-CD4 or anti-CD8 antibodies (BD Pharmingen) and flow cytometric sorting on a FACS ARIA flow cytometer (Becton Dickinson).

RT-PCR analysis

RNA was isolated using the Absolutely RNA RT-PCR Miniprep kit (Stratagene). One microgram of RNA was reverse-transcribed using an oligo-dT primer with the SuperScript First Strand Synthesis System (Invitrogen). Ten percent of the cDNA was subjected to PCR amplification (25 cycles of 94°C for 30 s, 58°C for 30 s, and 72°C for 1 min) for analysis of G2A, GPR4, or actin expression with the following primers: G2A, 5′-CTGCCTCAGGACTGGCTTGG and 3′-TCACACACGCAGAAATGGTGAC; GPR4, 5′-CTCTCTACATCTTCGTCATCGG and 3′-CGGTAGCACAGCAACATGAGTG; actin, 5′-CACAGGCATTGTGATGGACT and 3′-CTTCTGCATCCTGTCAGCCAA.

Mice

$G2A^{-/-}$ mice backcrossed a total of nine generations (N9) onto the C57BL/6J background were bred with C57BL/6J $LDLR^{-/-}$ mice (Jackson Laboratory, Bar Harbor, ME), and the resulting compound heterozygotes (N10 $G2A^{+/-}LDLR^{+/-}$) were intercrossed to obtain $G2A^{+/+}LDLR^{-/-}$ and $G2A^{-/-}LDLR^{-/-}$ progeny. Mice were weaned at 4 weeks of age and maintained on a standard rodent chow diet containing 4% fat (5015; Harlan Teklad, Madison, WI). At 8 weeks of age, mice were fasted for 12 h, weighed, bled by retro-orbital puncture, and transferred onto a "Western" diet (42% fat, 0.15% cholesterol, 19.5% casein without sodium cholate) (88137; Harlan Teklad) for 6 or 12 weeks. Mice were subsequently fasted for 12 h, weighed, and bled by retro-orbital puncture for lipid profile analysis.

Measurement of lipoprotein profiles and LPC levels

Plasma samples were processed for measurement of total cholesterol, unesterified cholesterol, HDL cholesterol, triglycerides,

and free fatty acids by enzymatic procedures described previously (20). Each sample was measured in triplicate, and Centers for Disease Control plasma samples with known lipid values were included as controls. LPC species were measured in snap-frozen aortas and plasma from five female LDLR$^{-/-}$ mice maintained on a regular chow diet or high-fat Western diet for 12 weeks by electrospray ionization-tandem mass spectrometry (ESI-MS/MS) as described previously (21, 22). Briefly, lipids were extracted from plasma or aortic tissue as described by Sutphen et al. (22) and resuspended in methanol-chloroform (2:1, v/v). Samples were spotted onto silica gel TLC plates and run in a solvent system composed of chloroform-methanol-ammonium hydroxide (65:35:5.5) with lipid standards (Avanti Polar Lipids). LPC bands were eluted from TLC plates, dried under nitrogen, and resuspended in 50 μl of methanol-water (1:1, v/v). To obtain standard curves, different amounts (5–300 pmol) of standard LPC solutions (6:0, 8:0, 10:0, 12:0, 14:0, 16:0, 18:0, 20:0, 22:0, and 24:0; Avanti Polar Lipids) were mixed with the same amount (50 pmol) of internal standard 17:0-LPC and ESI-MS/MS was performed using a Micromass Quattro II Triple Quadrupole Mass Spectrometer with a MassLynx data-acquisition system (Micromass, Inc., Beverly, MA). Peak intensity ratios (standard vs. internal standard) were plotted against molar ratios (standard vs. internal standard) to obtain standard curves. For quantitative analysis of LPC, 500 pmol of 17:0 LPC internal standard was added to each sample before lipid extraction. Lipid samples were delivered into the ESI source using a Waters 2690 autosampler (Waters, Milford, MA) in a mobile phase of methanol-water (1:1, v/v) and a flow rate of 100 μl/min. Parent scanning and MS/MS analyses were performed in the positive ion mode with multiple reaction monitoring and a dwell time of 100 ms using instrument settings identical to those described previously (22). Monitoring ions were at *m/z* 483 (parent ion) and 184 (product ion) for 16:0 lyso-PAF, 496 and 184 for 16:0-LPC, 510 and 184 for internal standard 17:0-LPC, 524 and 184 for 18:0-LPC, 522 and 184 for 18:1-LPC, 520 and 184 for 18:2-LPC, 544 and 184 for 20:4-LPC, and 568 and 184 for 22:6 LPC.

Atherosclerotic lesion quantification

After euthanization, the heart was perfused with 20 ml of PBS and removed by cutting at the proximal aorta. The upper portion of the heart was placed into a tissue mold, covered with OCT (Tissue-Tek), and frozen. Ventricular tissue was sectioned in a Leica 1850 cryostat, and serial 8 μm sections were collected onto microscope slides at the first appearance of the aortic valve leaflets. One hundred alternate sections were collected for lesion quantification, and intervening sections were collected and stored at −20°C for immunohistochemistry. Sections for lesion quantification were stained with Oil Red O and counterstained with hematoxylin and fast green. Lesion areas were measured morphometrically by two blinded independent observers with a Zeiss Axiostar Plus microscope using a 1 mm square eyepiece grid (100 × 10,000 μm^2) at 100× magnification.

Immunohistochemical analysis

One hundred alternate frozen sections were collected from each animal onto 25 slides (four sections per slide). For six randomly chosen mice from each of the four experimental groups (♀G2A$^{+/+}$LDLR$^{-/-}$, ♀G2A$^{-/-}$LDLR$^{-/-}$, ♂G2A$^{+/+}$LDLR$^{-/-}$, and ♂G2A$^{-/-}$LDLR$^{-/-}$), each of the four sections on six consecutive slides representing similar parts of the aortic root were stained with one of the following antibodies: *1*) rat anti-CD11b (BD Pharmingen); *2*) rat anti-CD3 (BD Pharmingen); *3*) rat anti-PECAM-1 (CD31) (BD Pharmingen); or *4*) rabbit anti-smooth muscle α-actin (Spring Biosciences, Fremont, CA). Sections were fixed in acetone at room temperature, treated with 0.3% hydrogen peroxide in PBS, and blocked in PBS containing 4% BSA and 10% serum of the species from which the secondary antibody was derived before incubation with primary antibodies. After incubation with appropriate biotinylated secondary antibodies (Vector Laboratories, Burlingame, CA) followed by HRP-conjugated streptavidin (Southern Biotechnology Associates), sections were developed with diaminobenzidine (Vector Laboratories) and counterstained with hematoxylin. The specificity of staining was confirmed using rat IgG_{2b} isotype control for CD11b and CD3, IgG_{2a} isotype control for PECAM-1, and rabbit IgG for smooth muscle α-actin. For T-cell quantification, CD3-positive cells were counted in lesions from each of the six randomly chosen ♀G2A$^{+/+}$LDLR$^{-/-}$, ♀G2A$^{-/-}$LDLR$^{-/-}$, ♂G2A$^{+/+}$LDLR$^{-/-}$, and ♂G2A$^{-/-}$LDLR$^{-/-}$ mice. For macrophage quantification, the percentage of total lesion area in each section occupied by CD11b-positive cells was measured morphometrically. For visualization of lesional collagen deposition, eight alternate 8 μm frozen sections from five randomly chosen animals of each experimental group were fixed in Bouin's fixative and stained with Masson's Trichrome (NewcomerSupply, Middleton, WI). The percentage of lesion area occupied by collagen was measured morphometrically.

Terminal deoxynucleotidyl transferase-mediated dUTP nick end labeling

For five randomly chosen female G2A$^{+/+}$LDLR$^{-/-}$ and G2A$^{-/-}$LDLR$^{-/-}$ mice, eight alternate 8 μm frozen sections from similar parts of the aortic root were fixed in 1% paraformaldehyde, permeabilized in cold ethanol-acetic acid (2:1, v/v) at −20°C, and subjected to terminal deoxynucleotidyl transferase-mediated dUTP nick end labeling (TUNEL) staining with or without terminal deoxynucleotidyl transferase using the ApopTag fluorescein in situ apoptosis detection kit (S7110; Chemicon International, Temecula, CA) according to the manufacturer's protocol. TUNEL-positive cells within lesions were quantified in color images captured on an Olympus BX60 fluorescence microscope. For colocalization of TUNEL staining with specific lesional cell types, aortic root sections were stained with anti-CD11b, anti-PECAM-1, or anti-CD3 antibodies followed by AlexaFluor-555-conjugated anti-rat antibody (BD Pharmingen).

RESULTS

G2A is expressed in cell types with key roles in atherosclerosis

GPR4 has been described as a second effector of LPC action (23). Therefore, we analyzed the expression of G2A and GPR4 in primary murine cell types involved in atherosclerosis (**Fig. 1**). By RT-PCR, we detected the expression of G2A in macrophages from various sources, T- and B-lymphocytes, bone marrow-derived mast cells and dendritic cells, and aortic endothelial cells. GPR4 expression was undetectable in these hematopoietic cell types and was found only in aortic endothelial cells. Finally, we detected no G2A or GPR4 expression in aortic smooth muscle cells. We also analyzed the same cell populations from G2A-deficient (G2A$^{-/-}$) mice to confirm the specificity of G2A amplification and detected no GPR4 expression in any of the G2A$^{-/-}$ hematopoietic cell types examined. Furthermore, there was no significant difference in GPR4 expression in G2A$^{-/-}$ aortic endothelial cells compared with their wild-type (G2A$^{+/+}$) counterparts (data not shown). Thus, there

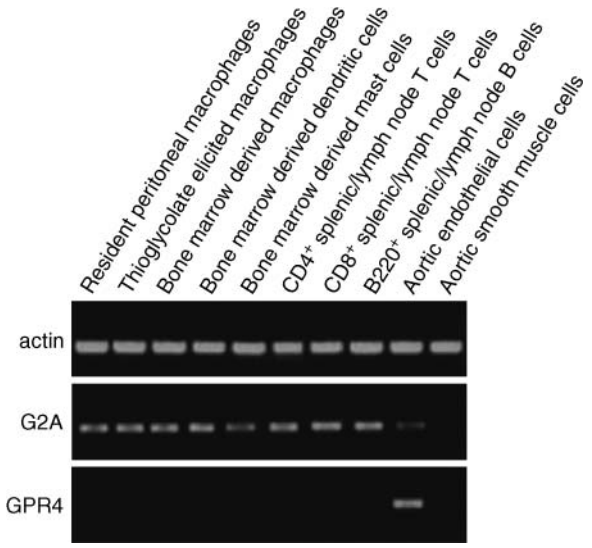

Fig. 1. G2A and G protein-coupled receptor 4 (GPR4) are expressed in key cell types involved in atherosclerosis. RT-PCR analysis was performed on total RNA from the indicated murine primary cells.

is no compensatory upregulation of GPR4 in the absence of G2A.

A recent study also reported GPR4 expression in endothelial cells and further suggested that GPR4 expression is transcriptionally induced by inflammatory stress in human vascular endothelial cells (24). However, this study did not detect G2A expression, which contradicts our observations. Although this may reflect the use of human versus murine cells, it is also possible that differences in their preparation, or immortalization in the case of cell lines, may influence endothelial cell receptor expression, as G2A is subject to transcriptional regulation by multiple stress stimuli (25). Furthermore, it is possible that endothelial cells from different vascular sites exhibit varying patterns of receptor expression (24). Nevertheless, our data show that G2A but not GPR4 is expressed in inflammatory cells, whereas GPR4 is the predominant receptor in aortic endothelial cells that also express lower levels of G2A.

LPC species are increased in atherosclerotic tissue and plasma of LDLR$^{-/-}$ mice

Of the major LPC species identified previously in human atherosclerotic tissue (26), only 16:0 LPC, 18:0 LPC, and 18:1 LPC have been shown to elicit cellular and molecular responses via G2A (6, 7, 9, 10). To determine whether these LPC species are significantly increased during atherogenesis in LDLR$^{-/-}$ mice, LPC levels were measured in plasma and the entire aorta of LDLR$^{-/-}$ mice before and after a 12 week period of high-fat Western diet intervention by ESI-MS/MS (21, 22). Levels of 16:0 lyso-PAF were measured and found to be increased significantly after Western diet intervention, confirming that a known product of PAF-AH hydrolysis was generated during atherogenesis (**Fig. 2**). Although levels of certain LPC species remained unchanged or were reduced by Western diet intervention in aortic tissue (18:2 LPC and 20:4 LPC) and plasma (18:0 LPC, 18:2 LPC, 20:4 LPC, and 22:6 LPC), several, including those previously established as major constituents of OxLDL (26), were increased significantly in atherosclerotic aortic tissue (16:0 LPC, 18:0 LPC, 18:1 LPC, and 22:6 LPC) and plasma (16:0 LPC and 18:1 LPC) (Fig. 2). Thus, atherosclerosis was associated with significant increases in the aorta of those LPC species (16:0 LPC, 18:0 LPC, and 18:1 LPC) capable of stimulating G2A-dependent chemotaxis, apoptosis, and other G2A-

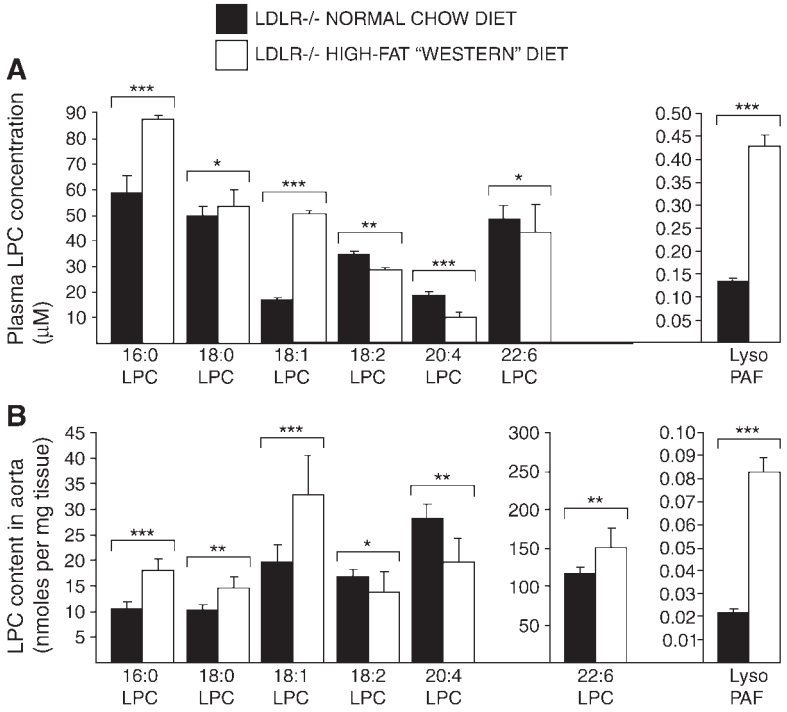

Fig. 2. Lysophosphatidylcholine (LPC) species that stimulate G2A-mediated responses are increased in the plasma and aortic tissue of low density lipoprotein receptor knockout (LDLR$^{-/-}$) mice after Western diet intervention. Concentrations of the indicated species of LPC in plasma samples (upper panel) and aortas (lower panel) of LDLR$^{-/-}$ mice maintained on a standard rodent chow diet or a high-fat Western diet for 12 weeks. PAF, platelet-activating factor. Statistical evaluation of LPC levels by unpaired Student's *t*-test: * $P > 0.05$, ** $P < 0.05$, *** $P < 0.01$. Error bars represent standard deviation.

mediated responses (6–11). Finally, loss of G2A function had no significant effect on the levels of any of the LPC species measured (data not shown), suggesting that G2A does not play a role in the clearance of LPC from the circulation.

Although we have no explanation for why aortic but not plasma levels of 18:0 LPC and 22:6 LPC species were increased during atherogenesis in LDLR$^{-/-}$ mice, several possibilities exist, including the generation of relevant oxidized *sn*-1 18:0 phosphatidylcholine decomposition substrates of PAF-AH at sufficient levels in atherosclerotic tissue only, the presence of blood-borne enzymes such as lysophospholipases that convert LPC to other lysophospholipids, as well as additional sources of 18:0 LPC in the circulation. Finally, myeloperoxidase (MPO)-generated reactive chlorinating species have been shown to promote oxidative cleavage of LDL plasmalogens, liberating α-chloro fatty aldehydes and unsaturated LPC species including 22:6 LPC in human atherosclerotic lesions (26, 27), suggesting that 22:6 LPC may have been generated in the aorta from plasmalogen phosphatidylcholine with a 22:6 acyl chain at the *sn*-2 position. However, MPO-derived products have not been detected in murine atherosclerotic tissue, consistent with the significantly lower levels of MPO in murine monocytes compared with their human counterparts (28). Furthermore, levels of 18:2 and 20:4 LPC species, major products of plasmalogen attack by MPO-derived reactive chlorinating species in human atherosclerotic tissue (26, 27), were not increased in LDLR$^{-/-}$ mice (Fig. 2). Therefore, similar studies with MPO-deficient atherogenic mice are required to determine the role of MPO-derived reactive chlorinating species plasmalogen attack in the generation of 22:6 LPC.

Loss of G2A does not affect lipid profiles during atherogenesis in LDLR$^{-/-}$ mice

LPC influences a variety of macrophage activities in vitro (5, 29, 30), although only chemotaxis has been directly shown to be stimulated via G2A (9). LPC stimulates chemotaxis and potentiates the inflammatory responses of T-cells via G2A in vitro (7, 8, 11), suggesting that this cell type may also be a major cellular effector of LPC action via G2A. To test whether these G2A-mediated effects are penetrant in vivo, we bred G2A$^{-/-}$ mice onto the atherosclerosis-susceptible LDLR$^{-/-}$ background. To avoid potentially confounding effects of genetic background, G2A$^{+/-}$LDLR$^{+/-}$ mice backcrossed onto the C57BL/6J strain for a total of 10 generations were intercrossed to derive all experimental animals. Male and female G2A$^{+/+}$LDLR$^{-/-}$ and G2A$^{-/-}$LDLR$^{-/-}$ mice were maintained on a high-fat Western diet for 12 weeks to induce atherosclerotic lesions in the aortic root. No significant differences in weight gain after the Western diet intervention were observed between G2A$^{+/+}$LDLR$^{-/-}$ and G2A$^{-/-}$ LDLR$^{-/-}$ mice of each gender (mean percentage weight gain after 12 weeks of Western diet intervention ± SD: ♀G2A$^{+/+}$LDLR$^{-/-}$, 28.9 ± 9.4%; ♀G2A$^{-/-}$LDLR$^{-/-}$, 29.8 ± 6.1%; ♂G2A$^{+/+}$LDLR$^{-/-}$, 56.6 ± 8.4%; ♂G2A$^{-/-}$LDLR$^{-/-}$, 58.3 ± 11.7%). Analysis of blood lipid profiles showed that the loss of G2A did not result in significant differences in plasma levels of LDL cholesterol, HDL cholesterol, unesterified cholesterol, triglycerides, and free fatty acids between gender-matched G2A$^{+/+}$LDLR$^{-/-}$ and G2A$^{-/-}$ LDLR$^{-/-}$ animals after the Western diet intervention (**Table 1**).

Loss of G2A function increases lesional macrophage content in LDLR$^{-/-}$ mice

To quantify atherosclerosis in G2A$^{+/+}$LDLR$^{-/-}$ and G2A$^{-/-}$LDLR$^{-/-}$ mice, we measured the area of lesions in serial frozen sections from the entire aortic root after 12 weeks of Western diet intervention. Morphometric quantification of lesion areas revealed no significant effect of G2A deficiency in male or female LDLR$^{-/-}$ mice (**Fig. 3A**). Furthermore, we observed no significant differences in lipid deposition in Oil Red O-stained lesions of G2A$^{+/+}$ LDLR$^{-/-}$ and G2A$^{-/-}$LDLR$^{-/-}$ mice irrespective of gender (Fig. 3B). Despite the development of similarly sized lesions in G2A$^{+/+}$LDLR$^{-/-}$ and G2A$^{-/-}$LDLR$^{-/-}$ mice, it was possible that their cellular composition may have been altered in the absence of G2A. Therefore, we performed immunohistochemical analysis of lesional inflammatory cell infiltration and morphology. Lesional staining of endothelial cells (PECAM-1) and smooth muscle cells (SMC α-actin) revealed no significant differences in morphology or extent of lesional penetration by either cell type irrespective of gender (**Fig. 4A**). However, by direct comparison of lesions from G2A$^{+/+}$LDLR$^{-/-}$ and G2A$^{-/-}$ LDLR$^{-/-}$ mice of each gender for CD11b-positive macrophage infiltration, we observed significant increases in lesion

TABLE 1. Loss of G2A does not affect plasma lipid profiles in LDLR$^{-/-}$ mice

Mice	LDL Cholesterol	HDL Cholesterol	Unesterified Cholesterol	Triglycerides	Fatty Acids
			mg/dl		
♀G2A$^{+/+}$LDLR$^{-/-}$ (n = 14)	1,053.4 ± 153.6	74.6 ± 20.3	317.8 ± 48	136.2 ± 47.4	61.6 ± 13.4
♀G2A$^{-/-}$LDLR$^{-/-}$ (n = 11)	1,106.8 ± 134.3	81.3 ± 20.1	332 ± 41.5	103.7 ± 33.1	54.8 ± 9.7
♂G2A$^{+/+}$LDLR$^{-/-}$ (n = 11)	1,104.8 ± 130.7	97.8 ± 20.1	339.7 ± 47.7	197.6 ± 55.1	68.1 ± 11.4
♂G2A$^{-/-}$LDLR$^{-/-}$ (n = 10)	1,038.1 ± 198.5	98.2 ± 20.0	311.1 ± 66.8	184.5 ± 68.4	62.3 ± 10.4

LDLR$^{-/-}$, low density lipoprotein receptor knockout. Indicated lipids were measured in plasma samples from G2A$^{+/+}$LDLR$^{-/-}$ and G2A$^{-/-}$LDLR$^{-/-}$ mice after 12 weeks of Western diet intervention. Values shown are means ± SD. Differences in plasma lipid levels of G2A$^{+/+}$LDLR$^{-/-}$ and G2A$^{-/-}$LDLR$^{-/-}$ mice of each gender are not statistically significant (unpaired Student's *t*-test: $P > 0.90$).

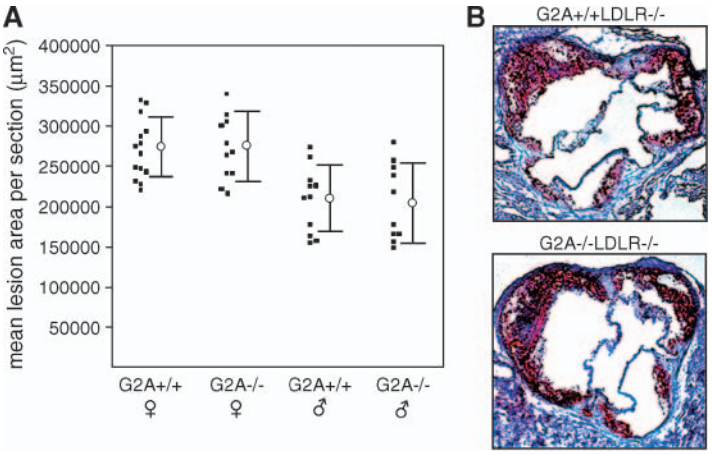

Fig. 3. Loss of G2A does not affect the size of developing atherosclerotic lesions in the aortic root of LDLR$^{-/-}$ mice. A: Mean lesion areas per section through the entire aortic root of the indicated LDLR$^{-/-}$ mice (squares). Average (circles) with SD (error bars) for each experimental group are shown alongside: ♀G2A$^{+/+}$LDLR$^{-/-}$, 274,390 ± 31,100 μm^2; ♀G2A$^{-/-}$ LDLR$^{-/-}$, 275,600 ± 43,900 μm^2; ♂G2A$^{+/+}$ LDLR$^{-/-}$, 209,800 ± 42,100 μm^2; ♂G2A$^{-/-}$LDLR$^{-/-}$, 204,900 ± 50,000 μm^2. B: Representative Oil Red O-stained sections of the aortic root of female G2A$^{+/+}$LDLR$^{-/-}$ and G2A$^{-/-}$LDLR$^{-/-}$ mice. Error bars represent standard deviation.

area occupied by macrophage-specific staining in G2A$^{-/-}$ LDLR$^{-/-}$ mice compared with their G2A$^{+/+}$LDLR$^{-/-}$ counterparts (Fig. 4A, D). Similarly, macrophage content was increased in early lesions of G2A$^{-/-}$LDLR$^{-/-}$ mice induced by a 6 week period of Western diet intervention (Fig. 4B).

Atherosclerotic lesions in G2A$^{+/+}$LDLR$^{-/-}$ and G2A$^{-/-}$ LDLR$^{-/-}$ mice contain similar numbers and distributions of T-cells

LPC stimulates chemotaxis of T-cells via G2A in vitro (7, 8, 11). Furthermore, loss of G2A function in T-cells is associated with hyperproliferative responses to T-cell receptor-

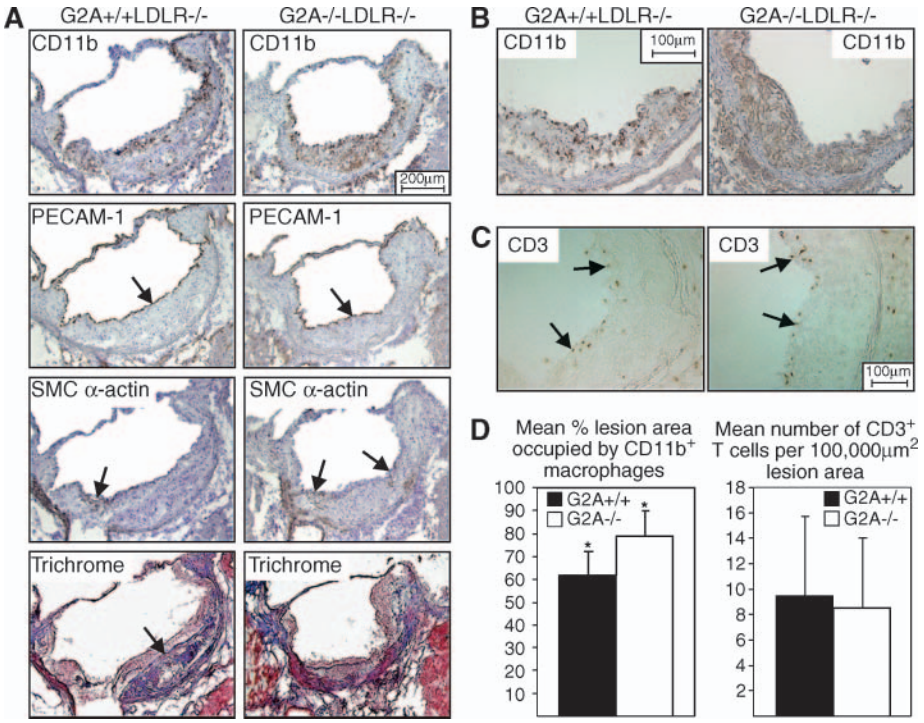

Fig. 4. G2A-mediated chemotactic responses of macrophages and T-cells are not manifested in vivo during atherosclerotic lesion development, and loss of G2A promotes lesional macrophage accumulation in LDLR$^{-/-}$ mice. A: Immunohistochemical and Masson's trichrome staining of consecutive aortic root sections of representative female G2A$^{+/+}$LDLR$^{-/-}$ and G2A$^{-/-}$LDLR$^{-/-}$ mice maintained on a Western diet for 12 weeks (CD11b, macrophages; PECAM-1, endothelial cells; SMC α-actin, smooth muscle cells). Arrows mark areas of immunoreactivity. The lower panels show Masson's trichrome staining of collagen (blue) in aortic root sections. B: Anti-CD11b immunohistochemical staining of aortic root sections from representative female G2A$^{+/+}$LDLR$^{-/-}$ and G2A$^{-/-}$LDLR$^{-/-}$ mice maintained on a Western diet for 6 weeks. C: Immunohistochemical staining of aortic root sections of representative female G2A$^{+/+}$LDLR$^{-/-}$ and G2A$^{-/-}$ LDLR$^{-/-}$ mice maintained on a Western diet for 12 weeks with a T-cell-specific antibody (CD3). D: Quantification of lesional macrophage and T-cell infiltration in female G2A$^{+/+}$LDLR$^{-/-}$ and G2A$^{-/-}$ LDLR$^{-/-}$ mice maintained on a Western diet for 12 weeks. Similar results were obtained with male G2A$^{+/+}$ LDLR$^{-/-}$ and G2A$^{-/-}$LDLR$^{-/-}$ mice. Unpaired Student's *t*-test: * $P < 0.05$. Error bars represent standard deviation.

dependent and T-cell receptor-independent stimuli (31), raising the possibility that lesional T-cells may be altered in G2A$^{-/-}$LDLR$^{-/-}$ mice. Immunohistochemical analysis revealed that lesions from G2A$^{+/+}$LDLR$^{-/-}$ and G2A$^{-/-}$LDLR$^{-/-}$ mice contained significant numbers of CD3-positive T-cells. However, we observed no significant differences in lesional T-cell numbers or distribution between G2A$^{+/+}$LDLR$^{-/-}$ and G2A$^{-/-}$LDLR$^{-/-}$ mice of either gender (Fig. 4C, D). Similarly, early lesions in G2A$^{+/+}$LDLR$^{-/-}$ and G2A$^{-/-}$LDLR$^{-/-}$ mice induced by a 6 week period of Western diet intervention contained comparable numbers of T-cells (data not shown).

Reduced numbers of lesional TUNEL-positive macrophages in G2A$^{-/-}$LDLR$^{-/-}$ mice

The ability of G2A to mediate the chemotactic action of LPC was not manifested in vivo, as lesional T-cell content was not altered in the absence of G2A and macrophage content was increased rather than decreased in G2A$^{-/-}$LDLR$^{-/-}$ mice compared with their G2A$^{+/+}$LDLR$^{-/-}$ counterparts. Because G2A has been shown to mediate the proapoptotic action of LPC (6), we investigated whether the loss of G2A-dependent apoptosis was responsible for this effect of G2A deficiency by performing TUNEL of aortic root lesions in G2A$^{+/+}$LDLR$^{-/-}$ and G2A$^{-/-}$LDLR$^{-/-}$ mice. We observed a significant decrease in the number of lesional TUNEL-positive cells in G2A$^{-/-}$LDLR$^{-/-}$ mice compared with their G2A$^{+/+}$ LDLR$^{-/-}$ counterparts (**Fig. 5A**, **B**). As G2A is expressed in macrophages, T-cells, and endothelial cells (Fig. 1), we performed immunofluorescent staining with cell-specific antibodies in conjunction with TUNEL to identify lesional apoptotic cells. TUNEL-positive cells were localized to areas of macrophage infiltration, and we observed no significant lesional T cell apoptosis at this stage of atherosclerotic lesion development (Fig. 5C). Therefore, increased lesional macrophage accumulation in G2A$^{-/-}$LDLR$^{-/-}$ mice is associated with the suppression of macrophage apoptosis during atherosclerotic lesion development.

Increased macrophage accumulation is associated with reduced lesional collagen content in G2A$^{-/-}$LDLR$^{-/-}$ mice

In addition to their central role in atherosclerotic lesion development, macrophages promote lesion destabilization by producing collagen and extracellular matrix-degrading enzymes, leading to weakening of the protective fibrous cap (32, 33). Therefore, increased macrophage

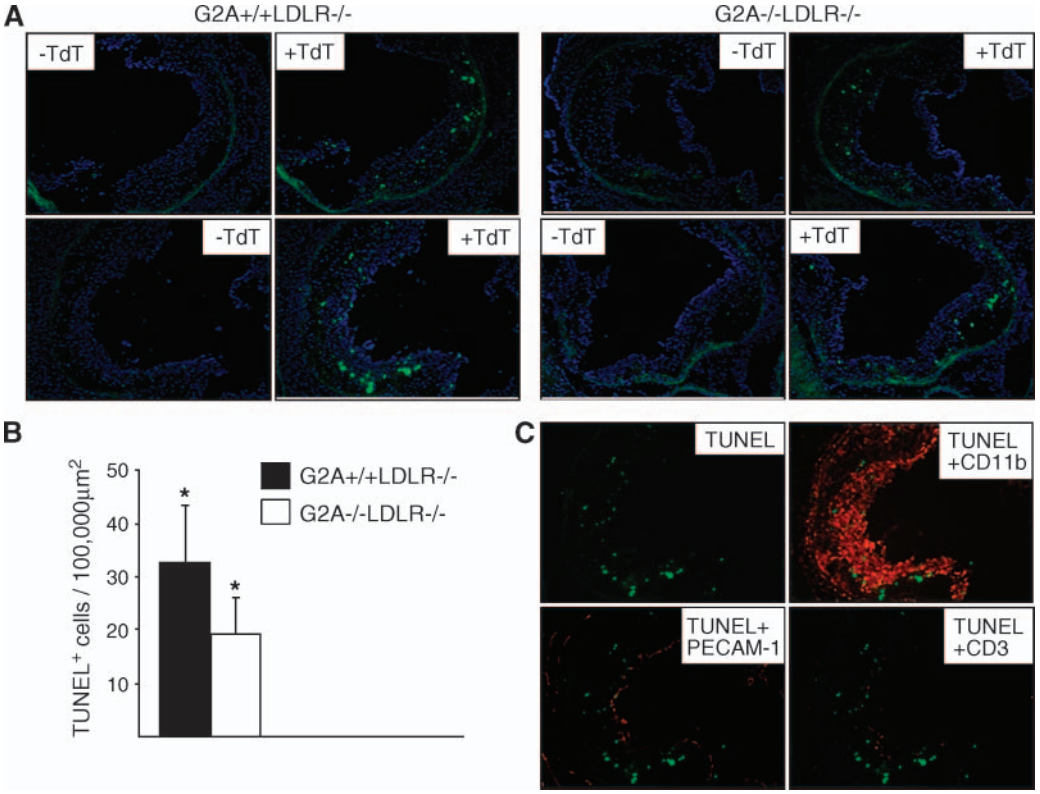

Fig. 5. Decreased apoptosis in atherosclerotic lesions of G2A$^{-/-}$LDLR$^{-/-}$ mice. A: Terminal deoxynucleotidyl transferase-mediated dUTP nick end labeling (TUNEL) staining (green) of representative aortic root lesions from female G2A$^{+/+}$LDLR$^{-/-}$ and G2A$^{-/-}$LDLR$^{-/-}$ mice maintained on a Western diet for 12 weeks. Control sections without terminal deoxynucleotidyl transferase staining (−TdT) demonstrate the specificity of TUNEL staining. The lesional boundary is identified by the autofluorescent elastic lamina (blue: nuclear 4′,6-diamidinophenylindole counterstain). B: Quantification of TUNEL-positive cells per 100,000 μm^2 lesion area in aortic root sections from G2A$^{+/+}$ LDLR$^{-/-}$ and G2A$^{-/-}$LDLR$^{-/-}$ mice. Unpaired Student's *t*-test: * $P < 0.05$. C: Immunofluorescent staining of a representative lesion from a female G2A$^{+/+}$LDLR$^{-/-}$ mouse with the indicated antibodies showing lesional apoptosis confined mostly to areas of macrophage infiltration. Error bars represent standard deviation.

numbers would be expected to reduce lesional collagen content. To determine whether macrophage accumulation in atherosclerotic lesions of G2A$^{-/-}$LDLR$^{-/-}$ mice was increased sufficiently to quantitatively or qualitatively alter collagen deposition, we subjected aortic root sections from G2A$^{+/+}$LDLR$^{-/-}$ and G2A$^{-/-}$LDLR$^{-/-}$ mice to Masson's trichrome staining. We consistently observed reductions in collagen content in lesions of G2A$^{-/-}$LDLR$^{-/-}$ mice compared with their G2A$^{+/+}$LDLR$^{-/-}$ counterparts (**Fig. 6**; see also Fig. 4A). As would be expected, those lesions with the greatest increases in macrophage-specific staining exhibited the greatest reductions in lesional collagen content (compare CD11b staining with the collagen staining of adjacent sections in Fig. 4A). However, most lesions (~90%) in G2A$^{-/-}$LDLR$^{-/-}$ mice displayed moderate reductions in overall collagen content characterized by less deposition within the shoulder region (Fig. 6A). Thus, macrophage content is increased sufficiently in the absence of G2A to reduce lesional collagen content despite having no impact on overall lesion size.

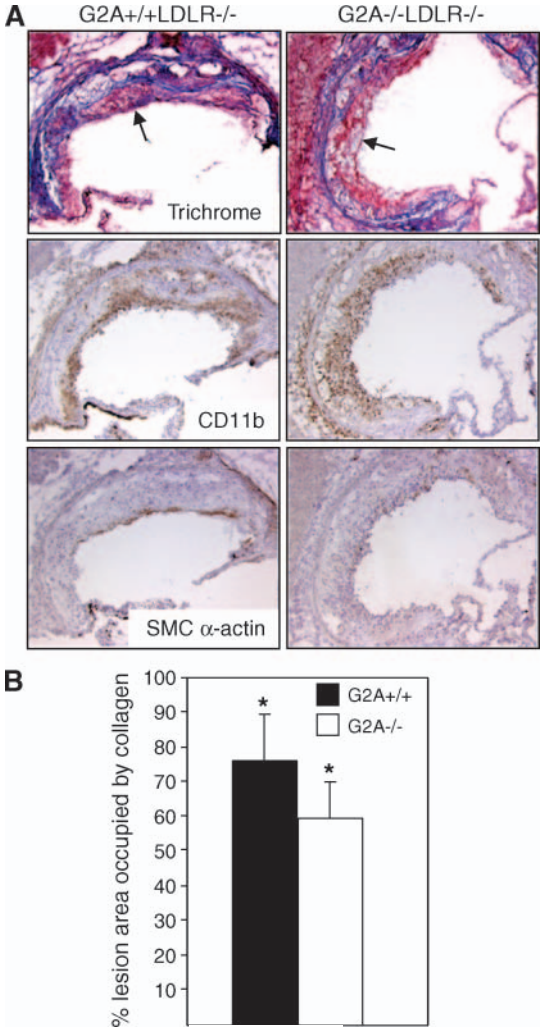

Fig. 6. Increased lesional macrophage accumulation is associated with decreased collagen content in G2A$^{-/-}$LDLR$^{-/-}$ mice. A: Masson's trichrome staining of collagen deposition (blue) and immunohistochemical staining of lesional macrophage and smooth muscle cell content in representative consecutive aortic root sections of female G2A$^{+/+}$LDLR$^{-/-}$ and G2A$^{-/-}$LDLR$^{-/-}$ mice maintained on a Western diet for 12 weeks. Note significantly increased lesional shoulder areas devoid of collagen in G2A$^{-/-}$LDLR$^{-/-}$ mice compared with their G2A$^{+/+}$LDLR$^{-/-}$ counterparts (arrows). SMC, smooth muscle cells. B: Quantification of the lesional area occupied by collagen in aortic root sections from G2A$^{+/+}$LDLR$^{-/-}$ and G2A$^{-/-}$LDLR$^{-/-}$ mice. Unpaired Student's *t*-test: * $P < 0.05$. Error bars represent standard deviation.

Our data show that despite the recognized G2A-mediated effects of LPC on chemotactic responses of macrophages and T-cells in vitro, they are not manifested in vivo in terms of lesional composition. Rather, the loss of G2A reduces apoptosis of macrophages and promotes their accumulation in atherosclerotic lesions of LDLR$^{-/-}$ mice, demonstrating that proapoptotic rather than chemotactic effects of G2A are most penetrant during atherosclerotic lesion development. Furthermore, increased lesional macrophage content in the absence of G2A is associated with reduced collagen content, suggesting that G2A may attenuate lesion destabilization.

DISCUSSION

Numerous reports describe LPC as a proinflammatory/proatherogenic factor based on its in vitro actions. However, most animal studies undertaken have revealed positive correlations rather than definitive evidence for a proatherogenic role (34, 35). By generating G2A-deficient LDLR$^{-/-}$ mice and examining how the loss of established G2A-mediated effects of LPC impact atherosclerotic lesion development and morphology, we have directly addressed one aspect of its pathophysiological role in atherosclerosis. Despite the generation of LPC species in atherosclerotic tissue capable of activating G2A-dependent responses during atherogenesis, the loss of G2A function in hypercholesterolemic LDLR$^{-/-}$ mice had no significant effect on atherosclerotic lesion size in the aortic root. Similar numbers of T-cells were present in lesions of G2A$^{+/+}$LDLR$^{-/-}$ and G2A$^{-/-}$LDLR$^{-/-}$ mice, and there was no evidence for a stimulatory effect of G2A on macrophage recruitment. Rather, we observed an increase in lesional macrophage numbers in G2A$^{-/-}$LDLR$^{-/-}$ mice compared with their G2A$^{+/+}$LDLR$^{-/-}$ counterparts, indicating the loss of G2A-mediated proapoptotic signaling (6). In support of this conclusion, we observed parallel reductions in the number of TUNEL-positive macrophages in atherosclerotic lesions of G2A$^{-/-}$LDLR$^{-/-}$ mice.

Macrophage accumulation and the subsequent production of proteolytic enzymes capable of degrading protective collagenous fibrous caps of advanced atherosclerotic lesions contributes to their destabilization and vulnerability to rupture (32, 33). Although most in vitro studies have shown that LPC elicits biological and signaling responses consistent with a proatherogenic role, its proapoptotic action on macrophages (30) suggests that it may also attenuate lesion destabilization by reducing lesional macrophage content. In support of this scenario, increased lesional

macrophage accumulation was associated with reduced collagen content in G2A$^{-/-}$LDLR$^{-/-}$ mice. Although macrophages could reduce lesional collagen content by promoting apoptosis of smooth muscle cells, a principal source of collagen synthesis and deposition (36), we did not observe any significant impact of G2A deficiency on lesional smooth muscle cell content or distribution. Therefore, it is more likely that increased levels of macrophage-derived collagen-degrading metalloproteinase activity are primarily responsible for the reduced collagen content of lesions in G2A$^{-/-}$LDLR$^{-/-}$ mice.

Although reduced collagen content is a characteristic of lesion instability, the promotion of macrophage survival in the absence of G2A would also be predicted to attenuate necrotic core formation, a beneficial effect reducing the thrombogenicity of the lesion. Furthermore, macrophage death is frequently observed in the shoulder regions of rupture-prone human plaques and may play an important role in murine models of plaque rupture (37, 38). Thus, suppression of macrophage apoptosis may also promote certain characteristics of plaque stabilization. Plaque rupture occurs frequently at specific sites such as the innominate/brachiocephalic arteries of apolipoprotein E-deficient mice (39), and this could be exploited to determine whether the degree to which macrophage death is suppressed in the absence of G2A promotes or attenuates plaque destabilization and susceptibility to rupture.

Decreased numbers of TUNEL-positive macrophages in G2A$^{-/-}$LDLR$^{-/-}$ mice may reflect a reduction in ongoing apoptosis that has significant impact during the course of lesion progression and is consistent with the loss of a recognized G2A-mediated effect of LPC (6). However, in the absence of definitive evidence that this effect is attributable to the loss of LPC-dependent G2A action, we cannot exclude a role for LPC-independent effects of G2A on apoptosis. In addition, other possible mechanisms by which G2A deficiency promotes lesional macrophage accumulation warrant consideration. For example, several studies support a role for G2A as a negative regulator of proliferation (25, 31, 40), suggesting that enhanced proliferation might contribute to the increased lesional macrophage content in the absence of G2A. It is also possible that G2A may regulate monocyte migratory potential within atherosclerotic lesions, as recent studies show that OxLDL and certain bioactive phospholipids implicated in promoting atherogenesis inhibit monocyte conversion into migratory cells with dendritic cell characteristics and thereby promote monocyte retention within atherosclerotic lesions (41, 42). These possibilities are currently being investigated in our laboratory.

The coexpression of G2A and GPR4 in aortic endothelial cells suggests possible functional redundancy with respect to LPC action during atherogenesis. However, G2A expression was not detected in endothelial cells from other sources (24), suggesting that G2A may be selectively expressed at particular vascular sites and/or subject to transcriptional regulation. Furthermore, there is controversy regarding the authenticity of GPR4 as a bona fide effector of LPC action, as recent studies did not detect LPC stimulation of membrane GTP binding and signal transduction in GPR4-overexpressing cell lines (43) and showed that GPR4 and related receptors, OGR1 and TDAG8, are activated by low extracellular pH rather than by LPC (16, 17, 19). Extracellular acidification was more recently reported to augment the production of inositol phosphate and the activation of the *zif268* promoter in human G2A-overexpressing cell lines, and the addition of LPC antagonized rather than potentiated inositol phosphate production (18). However, a subsequent study quantitatively comparing inositol phosphate and cAMP production by all four members of the "G2A family" in both receptor-overexpressing cell lines and primary immune cells from receptor-deficient mice demonstrated that the murine G2A receptor is insensitive to pH variations and that instead TDAG8 is a bona fide "pH-sensing" receptor in primary inflammatory cells (19). Cell lines overexpressing human G2A, on the other hand, exhibited only very weak induction of inositol phosphate and cAMP production in response to acidic pH (19). This may be explained by the absence of critical histidine residues in the predicted extracellular regions of G2A (19) known to be required for pH-dependent responses of OGR1 and TDAG8 and also present in GPR4 (16, 17). Although the pH at inflammatory sites may be reduced sufficiently to mediate GPR4, OGR1, and TDAG8 activation (44), the weak activation of human G2A compared with GPR4, OGR1, and TDAG8 by extracellular acidification nevertheless suggests a possible in vivo role for the human G2A receptor as a proton sensor regulating inflammatory responses under pathophysiological conditions. However, published data do not support a proton-sensing function for the murine G2A receptor; therefore, the effects of G2A deficiency reported in this article are unlikely to be attributable to the loss of pH-dependent responses.

The absence of a more robust effect of G2A deficiency in LDLR$^{-/-}$ mice not only supports the multifactorial nature of atherosclerosis but also reinforces the view that more penetrant effects of LPC are collectively mediated via G2A-independent as well as nonspecific mechanisms operating in multiple cell types during atherogenesis. For example, some effects of LPC may be the result of transient or lethal cell permeabilization (depending on the concentration of LPC) leading to cellular release of autocrine growth factors or apoptosis, respectively (45, 46). Additionally, the amphipathic nature of LPC results in its rapid nonspecific internalization through plasma membranes (47, 48), raising the possibility that some of its effects may be mediated intracellularly. For example, internalized LPC can induce macrophage apoptosis by inhibiting the rate-limiting enzyme of the de novo phosphatidylcholine biosynthetic pathway, CTP:phosphocholine cytidylyltransferase (47), and its reacylation by cytosolic acyltransferases promotes monocyte inflammatory responses to lipopolysaccharide (49–51). Our data nevertheless suggest that specific modulation of G2A activity in macrophages could provide a therapeutic approach to attenuate atherosclerotic lesion destabilization. However, this would require a complete understanding of the mechanism by which G2A

mediates LPC effects, a critical question that has recently reemerged after our failure to reproduce G2A/LPC binding originally reported in crude cell homogenates prepared from receptor-overexpressing cell lines (14, 15; our unpublished data). Therefore, LPC may activate G2A via a mechanism other than direct receptor binding at the cell surface, a scenario strongly supported by a recent study demonstrating that G2A-mediated responses to LPC, such as cell migration (7) and extracellular signal regulated kinase mitogen-activated protein kinase activation (14), are elicited by LPC-dependent mobilization of intracellular receptor pools to the plasma membrane (11). Importantly, as a proportion of ectopically expressed G2A is localized to the plasma membrane in the absence of exogenously added LPC, this study also provides a rational explanation for why certain G2A-dependent cell responses occur in an apparently "ligand-independent" manner in G2A-overexpressing cells (6, 12, 13).

An important question is whether G2A recycling to the plasma membrane is mediated by the interaction of internalized LPC with G2A or perhaps with a receptor-associated factor responsible for its retention within endosomes. Indeed, using cell fractionation and TLC phospholipid separation and quantification, we have observed rapid (<10 min) internalization of exogenously added LPC in live cells, preceding the effects of LPC on G2A redistribution reported by Wang et al. (11) (B. W. Parks and J. H. S. Kabarowski, unpublished data). Answers to this question may suggest novel approaches to control G2A receptor signaling that could be exploited to counteract deleterious or augment beneficial effects of LPC in atherosclerosis and other inflammatory diseases. The mechanism by which G2A mediates macrophage apoptosis and its impact on atherosclerosis at vascular sites other than those of predilection, therefore, are important goals of future studies. The roles of other putative effectors of LPC action, including those yet to be identified, must similarly be examined in the correct cellular context and at endogenous levels of expression. With this goal in mind, the generation of gene-targeted mice will allow functional studies to be performed in the context of physiological levels and kinetics of LPC production rather than of acute stimulation with doses of LPC that may not be physiologically relevant. These experimental approaches will thus establish how, if at all, individual effectors of LPC regulate atherosclerosis and the extent of functional redundancy among them. By gaining important mechanistic insights into the role of LPC in atherosclerosis, these studies will also provide a rational framework for the development of future treatments targeting inflammatory events driving atherosclerotic lesion progression.

The authors thank Owen Witte for providing $G2A^{-/-}$ mice, Xuping Wang and Hong Xiu Qi for advice on lesion analysis, Larry Castellani and Sarada Charugundla for lipid analyses, and Yi-jin Xiao and Yan Xu for LPC measurements. J.H.S.K. is a recipient of a Special Fellowship from the Leukemia and Lymphoma Society. A.J.L. is supported by National Institutes of Health Grant HL-30568 and the Laubisch Fund from the University of California, Los Angeles.

REFERENCES

1. Lusis, A. J. 2000. Atherosclerosis. *Nature.* **407:** 233–241.
2. Parthasarathy, S., and J. Barnett. 1990. Phospholipase A2 activity of low density lipoprotein: evidence for an intrinsic phospholipase A2 activity of apoprotein B-100. *Proc. Natl. Acad. Sci. USA.* **87:** 9741–9745.
3. Kume, N., H. Ochi, E. Nishi, M. A. Gimbrone, Jr., and T. Kita. 1995. Involvement of protein kinase C-independent mechanisms in endothelial ICAM-1 up-regulation by lysophosphatidylcholine. *Ann. N. Y. Acad. Sci.* **748:** 541–542.
4. Murugesan, G., M. R. Sandhya Rani, C. E. Gerber, C. Mukhopadhyay, R. M. Ransohoff, G. M. Chisolm, and K. Kottke-Marchant. 2003. Lysophosphatidylcholine regulates human microvascular endothelial cell expression of chemokines. *J. Mol. Cell. Cardiol.* **35:** 1375–1384.
5. Quinn, M. T., S. Parthasarathy, and D. Steinberg. 1988. Lysophosphatidylcholine: a chemotactic factor for human monocytes and its potential role in atherogenesis. *Proc. Natl. Acad. Sci. USA.* **85:** 2805–2809.
6. Lin, P., and R. D. Ye. 2003. The lysophospholipid receptor G2A activates a specific combination of G proteins and promotes apoptosis. *J. Biol. Chem.* **278:** 14379–14386.
7. Radu, C. G., L. V. Yang, M. Riedinger, M. Au, and O. N. Witte. 2004. T cell chemotaxis to lysophosphatidylcholine through the G2A receptor. *Proc. Natl. Acad. Sci. USA.* **101:** 245–250.
8. Han, K. H., K. H. Hong, J. Ko, K. S. Rhee, M. K. Hong, J. J. Kim, Y. H. Kim, and S. J. Park. 2004. Lysophosphatidylcholine up-regulates CXCR4 chemokine receptor expression in human CD4 T cells. *J. Leukoc. Biol.* **76:** 195–202.
9. Yang, L. V., C. G. Radu, L. Wang, M. Riedinger, and O. N. Witte. 2004. Gi-independent macrophage chemotaxis to lysophosphatidylcholine via the immunoregulatory GPCR G2A. *Blood.* **105:** 1127–1134.
10. Chen, G., J. Li, X. Qiang, C. J. Czura, M. Ochani, K. Ochani, L. Ulloa, H. Yang, K. J. Tracey, P. Wang, et al. 2005. Suppression of HMGB1 release by stearoyl lysophosphatidylcholine: an additional mechanism for its therapeutic effects in experimental sepsis. *J. Lipid Res.* **46:** 623–627.
11. Wang, L., C. G. Radu, L. V. Yang, L. A. Bentolila, M. Riedinger, and O. N. Witte. 2005. Lysophosphatidylcholine-induced surface redistribution regulates signaling of the murine G-protein-coupled receptor G2A. *Mol. Biol. Cell.* **16:** 2234–2247.
12. Kabarowski, J. H., J. D. Feramisco, L. Q. Le, J. L. Gu, S. W. Luoh, M. I. Simon, and O. N. Witte. 2000. Direct genetic demonstration of G alpha 13 coupling to the orphan G protein-coupled receptor G2A leading to RhoA-dependent actin rearrangement. *Proc. Natl. Acad. Sci. USA.* **97:** 12109–12114.
13. Zohn, I. E., M. Klinger, X. Karp, H. Kirk, M. Symons, M. Chrzanowska-Wodnicka, C. J. Der, and R. J. Kay. 2000. G2A is an oncogenic G protein-coupled receptor. *Oncogene.* **19:** 3866–3877.
14. Kabarowski, J. H., K. Zhu, L. Q. Le, O. N. Witte, and Y. Xu. 2001. Lysophosphatidylcholine as a ligand for the immunoregulatory receptor G2A. *Science.* **293:** 702–705.
15. Witte, O. N., J. H. Kabarowski, Y. Xu, L. Q. Le, and K. Zhu. 2005. Retraction. *Science.* **307:** 206.
16. Ludwig, M. G., M. Vanek, D. Guerini, J. A. Gasser, C. E. Jones, U. Junker, H. Hofstetter, R. M. Wolf, and K. Seuwen. 2003. Proton-sensing G-protein-coupled receptors. *Nature.* **425:** 93–98.
17. Wang, J. Q., J. Kon, C. Mogi, M. Tobo, A. Damirin, K. Sato, M. Komachi, E. Malchinkhuu, N. Murata, T. Kimura, et al. 2004. TDAG8 is a proton-sensing and psychosine-sensitive G-protein-coupled receptor. *J. Biol. Chem.* **279:** 45626–45633.
18. Murakami, N., T. Yokomizo, T. Okuno, and T. Shimizu. 2004. G2A is a proton-sensing G-protein coupled receptor antagonized by lysophosphatidylcholine. *J. Biol. Chem.* **279:** 42484–42491.
19. Radu, C. G., A. Nijagal, J. McLaughlin, L. Wang, and O. N. Witte. 2005. Differential proton sensitivity of related G protein-coupled receptors T cell death-associated gene 8 and G2A expressed in immune cells. *Proc. Natl. Acad. Sci. USA.* **102:** 1632–1637.
20. Hedrick, C. C., L. W. Castellani, C. H. Warden, D. L. Puppione, and

A. J. Lusis. 1993. Influence of mouse apolipoprotein A-II on plasma lipoproteins in transgenic mice. *J. Biol. Chem.* **268:** 20676–20682.
21. Xiao, Y., Y. Chen, A. W. Kennedy, J. Belinson, and Y. Xu. 2000. Evaluation of plasma lysophospholipids for diagnostic significance using electrospray ionization mass spectrometry (ESI-MS) analyses. *Ann. N. Y. Acad. Sci.* **905:** 242–259.
22. Sutphen, R., Y. Xu, G. D. Wilbanks, J. Fiorica, E. C. Grendys, Jr., J. P. LaPolla, H. Arango, M. S. Hoffman, M. Martino, K. Wakeley, et al. 2004. Lysophospholipids are potential biomarkers of ovarian cancer. *Cancer Epidemiol. Biomarkers Prev.* **13:** 1185–1191.
23. Zhu, K., L. M. Baudhuin, G. Hong, F. S. Williams, K. L. Cristina, J. H. Kabarowski, O. N. Witte, and Y. Xu. 2001. Sphingosylphosphorylcholine and lysophosphatidylcholine are ligands for the G protein-coupled receptor GPR4. *J. Biol. Chem.* **276:** 41325–41335.
24. Lum, H., J. Qiao, R. J. Walter, F. Huang, P. V. Subbaiah, K. S. Kim, and O. Holian. 2003. Inflammatory stress increases receptor for lysophosphatidylcholine in human microvascular endothelial cells. *Am. J. Physiol. Heart Circ. Physiol.* **285:** H1786–H1789.
25. Weng, Z., A. C. Fluckiger, S. Nisitani, M. I. Wahl, L. Q. Le, C. A. Hunter, A. A. Fernal, M. M. Le Beau, and O. N. Witte. 1998. A DNA damage and stress inducible G protein-coupled receptor blocks cells in G2/M. *Proc. Natl. Acad. Sci. USA.* **95:** 12334–12339.
26. Thukkani, A. K., J. McHowat, F. F. Hsu, M. L. Brennan, S. L. Hazen, and D. A. Ford. 2003. Identification of {alpha}-chloro fatty aldehydes and unsaturated lysophosphatidylcholine molecular species in human atherosclerotic lesions. *Circulation.* **108:** 3128–3133.
27. Thukkani, A. K., C. J. Albert, K. R. Wildsmith, M. C. Messner, B. D. Martinson, F. F. Hsu, and D. A. Ford. 2003. Myeloperoxidase-derived reactive chlorinating species from human monocytes target plasmalogens in low density lipoprotein. *J. Biol. Chem.* **278:** 36365–36372.
28. Brennan, M. L., M. M. Anderson, D. M. Shih, X. D. Qu, X. Wang, A. C. Mehta, L. L. Lim, W. Shi, S. L. Hazen, J. S. Jacob, et al. 2001. Increased atherosclerosis in myeloperoxidase-deficient mice. *J. Clin. Invest.* **107:** 419–430.
29. Sakai, M., A. Miyazaki, H. Hakamata, Y. Sato, T. Matsumura, S. Kobori, M. Shichiri, and S. Horiuchi. 1996. Lysophosphatidylcholine potentiates the mitogenic activity of modified LDL for human monocyte-derived macrophages. *Arterioscler. Thromb. Vasc. Biol.* **16:** 600–605.
30. Carpenter, K. L., I. F. Dennis, I. R. Challis, D. P. Osborn, C. H. Macphee, D. S. Leake, M. J. Arends, and M. J. Mitchinson. 2001. Inhibition of lipoprotein-associated phospholipase A2 diminishes the death-inducing effects of oxidised LDL on human monocyte-macrophages. *FEBS Lett.* **505:** 357–363.
31. Le, L. Q., J. H. Kabarowski, Z. Weng, A. B. Satterthwaite, E. T. Harvill, E. R. Jensen, J. F. Miller, and O. N. Witte. 2001. Mice lacking the orphan G protein-coupled receptor G2A develop a late-onset autoimmune syndrome. *Immunity.* **14:** 561–571.
32. Galis, Z. S., G. K. Sukhova, M. W. Lark, and P. Libby. 1994. Increased expression of matrix metalloproteinases and matrix degrading activity in vulnerable regions of human atherosclerotic plaques. *J. Clin. Invest.* **94:** 2493–2503.
33. Libby, P., and M. Aikawa. 2002. Stabilization of atherosclerotic plaques: new mechanisms and clinical targets. *Nat. Med.* **8:** 1257–1262.
34. Ivandic, B., L. W. Castellani, X. P. Wang, J. H. Qiao, M. Mehrabian, M. Navab, A. M. Fogelman, D. S. Grass, M. E. Swanson, M. C. de Beer, et al. 1999. Role of group II secretory phospholipase A2 in atherosclerosis. 1. Increased atherogenesis and altered lipoproteins in transgenic mice expressing group IIa phospholipase A2. *Arterioscler. Thromb. Vasc. Biol.* **19:** 1284–1290.
35. Webb, N. R., M. A. Bostrom, S. J. Szilvassy, D. R. van der Westhuyzen, A. Daugherty, and F. C. de Beer. 2003. Macrophage-expressed group IIA secretory phospholipase A2 increases atherosclerotic lesion formation in LDL receptor-deficient mice. *Arterioscler. Thromb. Vasc. Biol.* **23:** 263–268.
36. Kockx, M. M., and A. G. Herman. 1998. Apoptosis in atherogenesis: implications for plaque destabilization. *Eur. Heart J.* **19 (Suppl. G):** 23–28.
37. Rosenfeld, M. E., P. Polinsky, R. Virmani, K. Kauser, G. Rubanyi, and S. M. Schwartz. 2000. Advanced atherosclerotic lesions in the innominate artery of the ApoE knockout mouse. *Arterioscler. Thromb. Vasc. Biol.* **20:** 2587–2592.
38. Johnson, J. L., and C. L. Jackson. 2001. Atherosclerotic plaque rupture in the apolipoprotein E knockout mouse. *Atherosclerosis.* **154:** 399–406.
39. Rosenfeld, M. E., K. G. Carson, J. L. Johnson, H. Williams, C. L. Jackson, and S. M. Schwartz. 2002. Animal models of spontaneous plaque rupture: the holy grail of experimental atherosclerosis research. *Curr. Atheroscler. Rep.* **4:** 238–242.
40. Le, L. Q., J. H. Kabarowski, S. Wong, K. Nguyen, S. S. Gambhir, and O. N. Witte. 2002. Positron emission tomography imaging analysis of G2A as a negative modifier of lymphoid leukemogenesis initiated by the BCR-ABL oncogene. *Cancer Cell.* **1:** 381–391.
41. Llodra, J., V. Angeli, J. Liu, E. Trogan, E. A. Fisher, and G. J. Randolph. 2004. Emigration of monocyte-derived cells from atherosclerotic lesions characterizes regressive, but not progressive, plaques. *Proc. Natl. Acad. Sci. USA.* **101:** 11779–11784.
42. Angeli, V., J. Llodra, J. X. Rong, K. Satoh, S. Ishii, T. Shimizu, E. A. Fisher, and G. J. Randolph. 2004. Dyslipidemia associated with atherosclerotic disease systemically alters dendritic cell mobilization. *Immunity.* **21:** 561–574.
43. Bektas, M., L. S. Barak, P. S. Jolly, H. Liu, K. R. Lynch, E. Lacana, K. B. Suhr, S. Milstien, and S. Spiegel. 2003. The G protein-coupled receptor GPR4 suppresses ERK activation in a ligand-independent manner. *Biochemistry.* **42:** 12181–12191.
44. Lardner, A. 2001. The effects of extracellular pH on immune function. *J. Leukoc. Biol.* **69:** 522–530.
45. Chai, Y. C., D. G. Binion, R. Macklis, and G. M. Chisolm 3rd. 2002. Smooth muscle cell proliferation induced by oxidized LDL-borne lysophosphatidylcholine. Evidence for FGF-2 release from cells not extracellular matrix. *Vascul. Pharmacol.* **38:** 229–237.
46. Kogure, K., S. Nakashima, A. Tsuchie, A. Tokumura, and K. Fukuzawa. 2003. Temporary membrane distortion of vascular smooth muscle cells is responsible for their apoptosis induced by platelet-activating factor-like oxidized phospholipids and their degradation product, lysophosphatidylcholine. *Chem. Phys. Lipids.* **126:** 29–38.
47. Boggs, K. P., C. O. Rock, and S. Jackowski. 1995. Lysophosphatidylcholine and 1-O-octadecyl-2-O-methyl-rac-glycero-3-phosphocholine inhibit the CDP-choline pathway of phosphatidylcholine synthesis at the CTP:phosphocholine cytidylyltransferase step. *J. Biol. Chem.* **270:** 7757–7764.
48. Van Der Luit, A. H., M. Budde, M. Verheij, and W. J. Van Blitterswijk. 2003. Different modes of internalization of apoptotic alkyl-lysophospholipid and cell-rescuing lysophosphatidylcholine. *Biochem. J.* **374:** 747–753.
49. Boggs, K. P., C. O. Rock, and S. Jackowski. 1995. Lysophosphatidylcholine attenuates the cytotoxic effects of the antineoplastic phospholipid 1-O-octadecyl-2-O-methyl-rac-glycero-3-phosphocholine. *J. Biol. Chem.* **270:** 11612–11618.
50. Chambers, K., and W. J. Brown. 2004. Characterization of a novel CI-976-sensitive lysophospholipid acyltransferase that is associated with the Golgi complex. *Biochem. Biophys. Res. Commun.* **313:** 681–686.
51. Schmid, B., M. J. Finnen, J. L. Harwood, and S. K. Jackson. 2003. Acylation of lysophosphatidylcholine plays a key role in the response of monocytes to lipopolysaccharide. *Eur. J. Biochem.* **270:** 2782–2788.